RSC Advances

ROYAL SOCIETY OF CHEMISTRY

www.rsc.org/advances

Journal Name

RSCPublishing

ARTICLE

Cite this: DOI: 10.1039/x0xx00000x

Received 00th January 2014,
Accepted 00th January 2014

DOI: 10.1039/x0xx00000x

www.rsc.org/

Synthesis of novel chiral L-leucine grafted PEDOT derivatives with excellent electrochromic performances

Dufen Hu†, Baoyang Lu†, Xuemin Duan*, Jingkun Xu*, Long Zhang, Kaixin Zhang, Shimin Zhang and Shijie Zhen

Two amino acid-functionalized poly(3,4-ethylenedioxythiophene) (PEDOT) derivatives, poly(*N*-(*tert*-butoxycarbonyl)-L-leucyl(3,4-ethylenedioxythiophene-2'-yl)methylamide) (PEDOT-Boc-Leu) and poly(L-leucyl(3,4-ethylenedioxythiophene-2'-yl)methylamide) (PEDOT-Leu) were synthesized electrochemically via potentiostatic polymerization of corresponding monomers *N*-(*tert*-butoxycarbonyl)L-leucyl(3,4-ethylenedioxythiophene-2'-yl)methylamide (EDOT-Boc-Leu) and L-leucyl(3,4-ethylenedioxythiophene-2'-yl)methylamide (EDOT-Leu), which were synthesized by grafting Boc-L-leucine and L-leucine into 3,4-ethylenedioxythiophene (EDOT) side chain. The electrochemical behaviors, structural characterization, circular dichroism, spectroscopic properties, surface morphology, electrochromic properties and thermal stabilities of PEDOT-Boc-Leu and PEDOT-Leu films were systematically investigated. These L-leucine grafted PEDOT derivatives displayed excellent reversible redox activities, rough and compact surface, and good thermal stability. The circular dichroism spectra suggested the chirality of these polymers. Importantly, the introduction of L-leucine group enhanced electrochromic properties of PEDOT and resulted in high contrast ratios ($\Delta T\%$ = 49% at 600 nm for PEDOT-Boc-Leu) and high coloration efficiencies (431 cm^2 C^{-1} at 960 nm for PEDOT-Leu). Satisfactory results implied that the obtained polymer films can probably be further developed in various applications, such as electrochromic devices, optical displays and chiral recognition.

Introduction

Chiral conducting polymers, as an important branch of conducting polymers, have been paid high attention by many researchers and are widely used in many areas such as chiral sensors, chiral catalysts, and chromatographic separation of enantiomeric drugs.[1-3] Chiral conducting polymers not only exhibit remarkable redox properties,[4] pH switching capabilities, relative ease of synthesis,[5] and exceptional chiroptical performance,[6] but also show high electrical conductivity and good environmental stability. Based on above advantages, chiral conducting polymers are identified as possessing a great number of exciting new potential applications,[7] such as chiral sensors,[8] separation of enantiomers,[9] electrochemical asymmetric synthesis,[10] and chiral catalysts.[11] Up to date, several methods have been proposed to prepare chiral conducting polymers, including the polymerization of corresponding chiral monomers,[12-16] asymmetric selective polymerization,[17,18] and the introduction of a chiral group onto an achirality polymer via chemical reactions.[19] Kazuo Akagi and co-workers[20-30] have developed an electrochemical polymerization method with chiral nematic liquid crystal as an electrolyte, and successfully use the method to produce unsubstituted chiral conducting polymers. More recently, a series of new-generation chiral conducting polymers have been designed and synthesized by introducing chiral moiety into the side chains of conducting polymers,[31-34] which is a fashionable approach to obtain chiral conducting polymers, and some promising applications are presented.

Among various kinds of conducting polymers, poly(3,4-ethylenedioxythiophene) (PEDOT) is one of representative and highly promising conducting polymers with versatile properties such as high electrical conductivity, low band gap, good redox activity, thermal stability, long-term stability, and excellent transparency in the doped state.[20,35] Also PEDOT is applied in a variety of areas, such as electrolytic capacitors,[36] printed wiring boards,[37,38] ITO substitution,[39] antistatic coatings,[40-42] electroluminescent lamps,[43-45] organic solar cells,[46,47] electrochromics,[48-50] and so on.[51,52] Unfortunately, PEDOT shows poor photophysical property in the whole visible region and chiral property,[53] which limits its wide application as optoelectronics and chiral materials. In comparison with PEDOT, chiral PEDOT derivatives display chiroptical properties and helical structures and thus show significant academic research value and application prospect. Also, the electrochromic behavior of chiral PEDOT derivatives is superior to other chiral π-conjugated polymers without electrochemical activity.[54] In addition, the chirality of the polymer can be controlled by changing the polymer structures between the doped and dedoped states through electrochemical doping and dedoping processes.[24] Yet to date, advanced work has been done to study chiral PEDOT derivatives by different research groups,[15,20,21,24,55-59] but the design and synthesis of novel PEDOT derivatives with extraordinary photophysical and excellent chiral properties are still very necessary and significant, which apparently is a considerable challenge.

As the basic composition unit of macromolecular protein, chiral amino acids are not only biologically important to life but also play crucial roles as chiral auxiliaries and building blocks in organic synthesis.[60] Furthermore, all nature amino acids show excellent biocompatibility, low toxicity, efficient and quick biodegradability, which is beneficial for the fabrication of sensing platform. Hence, the natural amino acids can be used as the ideal chiral materials for the design and synthesis of chiral PEDOTs by attaching onto their side chain.[61]

In this work, L-leucine was chosen as the side chain moiety onto EDOT through covalent bonding. Two novel PEDOT derivatives, poly(*N*-(*tert*-butoxycarbonyl)-L-leucyl(3,4-ethylenedioxythiophene-2'-yl) methylamide) (PEDOT-Boc-Leu) and poly(L-leucyl(3,4-ethylenedioxythiophene-2'-yl)methylamide) (PEDOT-Leu), were electrosynthesized for the first time through the electropolymerization of corresponding EDOT derivatives of *N*-(*tert*-butoxycarbonyl)-L-leucyl(3,4-ethylenedioxythiophene-2'-yl)methylamide (EDOT-Boc-Leu) and L-leucyl(3,4-ethylenedioxythiophene-2'-yl)methylamide (EDOT-Leu), which were synthesized by acylation reaction. The electrochemical behavior, structural characterization, circular dichroism, solubility, spectroscopic properties, thermal stabilities, and surface morphology of as-prepared PEDOT-Boc-Leu and PEDOT-Leu films and their electrochromic properties were investigated in detail.

Experimental section

Materials

L-leucine (99%), triphenylphosphine (PPh_3, 99%), sodium azide (NaN_3, 99%); N_3-dimethylpropane-1,3-diamine (EDC, 99%), *N*-hydroxybenzotrizole (HOBT, 99%), trifluoroacetic acid (TFA, 99%), and di-*tert*-butyl dicarbonate ($(Boc)_2O$, 99%) were purchased from Aladdin Chemistry Co. Ltd. and dimethyl sulfoxide (DMSO, AR) was purchased from Tianjin Bodi Chemicals Co., Ltd. All above of reagents were used as received. Dichloromethane (CH_2Cl_2, AR; Tianjin Damao Chemical Reagent Factory) was purified by distillation over calcium hydride before used. Tetra-n-butylammonium hexafluorophosphate (Bu_4NPF_6, 99%; Acros Organics) was dried under vacuum at 60 °C for 24 h before used. 2'-Chloromethyl-3,4-ethylenedioxythiophene (EDOT-MeCl) was prepared in accordance with Duan et al.[62,63]

Syntheses

2.2.1 2'-Azidomethyl-3,4-ethylenedioxythiophene (EDOT-MeN_3)[64]

Under a nitrogen atmosphere, EDOT-MeCl (0.17 g, 0.9 mmol) and NaN_3 (0.08 g, 1.2 mmol) were dissolved in DMF (10 mL) and stirred at 120 °C for 17 h. After cooling, 10 mL H_2O was added. Then the mixture was extracted with ethyl acetate (5 × 15 mL). The organic phases were combined and extracted with H_2O (3 × 15 mL) and brine (1 × 15 mL), dried with anhydrous $MgSO_4$, and filtered. After evaporation of the solvent, the remaining crude product was isolated by flash chromatography (silica gel, petroleum ether/ethyl acetate, 10/1, v/v) to give 0.16 g of a light yellow oil (yield 91%). ^{1}H NMR (400 MHz, $CDCl_3$, ppm): δ 6.37 (dd, J_1 = 3.6 Hz, J_2 = 11.2 Hz, 2H), 4.03-4.34 (m, 3H), 3.47-3.60 (m, 2H).

2'-Aminiomethyl-3,4-ethylenedioxythiophene (EDOT-MeNH$_2$)[65]

EDOT-MeN$_3$ (0.20 g, 1 mmol) and PPh$_3$ (0.29 g, 1.1 mol) in a molar ration of 1:1.1 were dissolved in 4.5 mL THF and stirred at 50 °C. Then, NaOH (4.5 mL, 2 M) was added dropwise, and the reaction mixture was stirred overnight. The reaction mixture was allowed to cool to room temperature. After evaporation of THF, 2 M HCl solution was used to control the pH below 3. Then the aqueous layer was extracted with CH_2Cl_2 and the combined organic layers were discarded. 1 M NaOH solution was added to adjust the pH of aqueous layer to 8. The aqueous layer was extracted with CH_2Cl_2 and the combined organic layers were dried with anhydrous $MgSO_4$. After evaporation of the solvent, the remaining crude product was isolated by flash chromatography (silica gel, dichloromethane/methanol, 20/1, v/v) to give 0.15 g of a colorless oil (yield 87%). ^{1}H NMR (400 MHz, $CDCl_3$, ppm): δ 6.35 (d, J = 4 Hz, 2H), 3.99-4.24 (m, 3H), 2.96-3.03 (m, 2H), 1.52 (s, 2H).

***N*-(tert-butoxycarbonyl)-L-leucine (*N*-Boc-L-Leu)**

A solution of $(Boc)_2O$ (2.59 g, 11.87 mmol) in dioxane (9 mL) was added to an ice-cold solution of L-leucine (1.31 g, 10.00 mmol) in 1 M NaOH (20 mL) with stirring at -5 °C. After 30 min, then the mixture was stirred for over 14 h at to room temperature. The mixture was concentrated to half its original volume by rotary evaporation, cooled in ice, and acidified pH to 2-3 by slow addition of 1 M $NaHSO_4$. Finally, the solution was extracted with acetic ether (3 × 20 mL), the combined organic layer were dried with anhydrous $MgSO_4$, and concentrated to give 1.86 g of a colorless solid (yield 51%).

EDOT-Boc-Leu

EDOT-MeNH$_2$ (0.37 g, 2.16 mmol), EDC (0.47 g, 2.38 mmol), and HOBT (0.03 g, 0.22 mmol) were dissolved in CH_2Cl_2 (15 mL) with stirring while being cooled in an ice bath. A solution of *N*-Boc-L-Leu (0.55 g, 0.24 mmol) in CH_2Cl_2 (5 mL) was added slowly. After stirring for 1 h, the ice bath was removed and the reaction was performed with continued stirring at room temperature for another 16 h. Subsequently, the colorless reaction solution was washed with 1 M HCl (3 × 30 mL), a saturated solution of $NaHCO_3$ (3 × 30 mL), and then with saturated brine (1 × 30 mL), respectively. The organic layer was dried with anhydrous $MgSO_4$. The solvent was removed under reduced pressure and the remaining crude product was isolated by flash chromatography (silica gel, petroleum ether/ethyl acetate, 2/1, v/v) to give 0.79 g of a colorless solid (yield 95%). $[\alpha]^{20}$ = -14.87º. ^{1}H NMR (400 MHz, DMSO-d_6, ppm): δ 8.10 (t, J = 7.6 Hz, 1H), 6.90 (s, 1H), 6.56 (d, J = 2.8 Hz, 2H), 4.18 (d, J = 12 Hz, 2H), 3.84-3.92 (m, 2H), 3.36 (d, J = 17.6 Hz, 2H), 1.58 (s, 1H), 1.35-1.43(m, 11H), 0.85 (t, J = 7.2 Hz, 6H).

EDOT-Leu[66]

EDOT-Boc-Leu (0.80 g, 2.08 mmol) was dissolved in CH_2Cl_2 (38 mL) with stirring while being cooled in an ice bath. A solution of TFA (2 mL) in CH_2Cl_2 (2 mL) was added slowly. After 4-5 h, the pH of the mixture was adjusted to basicity with a saturated solution of $NaHCO_3$. Then the mixture was extracted with CH_2Cl_2 (3 × 120 mL), and saturated brine (3 × 120 mL), respectively. The organic layer was dried with anhydrous $MgSO_4$. The solvent was removed under reduced pressure and the remaining crude product was isolated by flash chromatography (silica gel, dichloromethane/methanol, 32/1, v/v) to give 0.38 g of a colorless solid (yield 64%). $[\alpha]^{20}$ = -10.88º. ^{1}H NMR (400 MHz, $CDCl_3$, ppm): δ 7.70 (s, 1H), 6.25 (s, 2H), 4.11-4.20 (m, 2H), 3.81-3.88 (m, 1H), 3.33-3.60 (m, 3H), 1.62-1.66 (m, 2H), 1.44 (s, 2H), 1.23-1.31 (m, 1H), 0.83-0.89 (m, 6H).

Electrochemical measurements

Electrochemical synthesis and examinations were performed in a one-compartment cell with the use of Model 263 potentiostat-galvanostat (EG&G Princeton Applied Research) under a computer control. The three electrodes of the working electrode, the reference electrode, and the counter electrode were all platinum (Pt) wires with a diameter of 0.5 mm, which were placed 5 mm apart in the transverse direction during the measurements (Scheme 1). Besides, to obtain a sufficient amount of polymer for characterization, the Pt sheets with a surface area of 10 and 12 cm^2 each (10 mm apart) were employed as working and counter electrodes, respectively. The Pt wire electrode directly immersed in the solution served as the reference electrode and it also revealed sufficient stability during the experiments. Electrodes mentioned above were carefully polished with abrasive paper (1500 mesh), and ultrasonic cleaned by water and acetone successively before each examination. All experiments were carried out under a slight argon overpressure. Finally, the polymer films were dried at 60 °C under vacuum for 24 h. The PEDOT-Boc-Leu film was prepared in CH_2Cl_2-Bu_4NPF_6 (0.10 M) containing 0.01 M EDOT-Boc-Leu and characterized electrochemically in monomer-free CH_2Cl_2-Bu_4NPF_6 (0.10 M). The PEDOT-Leu film was prepared in CH_2Cl_2-Bu_4NPF_6 (0.10 M) containing 5% TFA and 0.01 M EDOT-Leu and characterized electrochemically in monomer-free CH_2Cl_2-Bu_4NPF_6 (0.10 M) containing 5% TFA. Both PEDOT-Boc-Leu and PEDOT-Leu films were dedoped by 25% ammonia for three days. After dedoping, their color both changed to brownish yellow

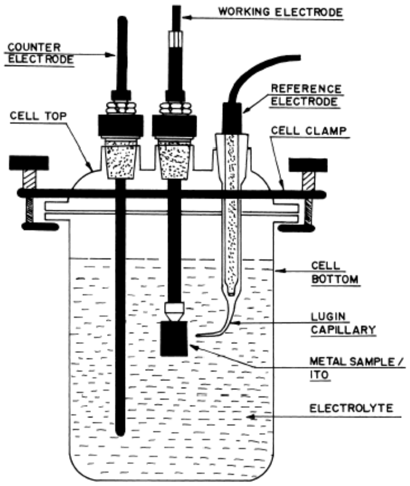

Scheme 1. The three-electrode system employed for electrochemical polymerization and tests.

Characterization

NMR spectra were recorded on a Bruker AV 400 NMR spectrometer with d_6-DMSO or $CDCl_3$ as the solvent and tetramethylsilane as an internal standard (TMS, singlet, chemical shift: 0.0 ppm). Infrared spectra (IR) were recorded using Bruker Vertex 70 Fourier spectrometer with samples in KBr pellets. Ultraviolet-visible (UV-*vis*) spectra were measured with a Perkin-Elmer Lambda 900 ultraviolet-visible-near-infrared spectrophotometer. Optical rotation determination was performed on Anton Paar MCP 200 polarimeter. Fluorescence spectra of the monomers and polymers were determined with an F-4500 fluorescence spectrophotometer (Hitachi). Thermogravimetric (TG) and differential thermogravimetric (DTG) analyses were performed with a Pyris Diamond TG/DTA thermal analyzer (Perkin-Elmer). Circular dichroism (CD) was measured with JASCO Corp., J-810, Rev. 1.00. Scanning electron microscopy (SEM) measurements were taken using Sigma cold field emission scanning electron microscope. The addition of solutions to the cell was performed with the Finnpipette (Labsystems, Helsinki, Finland). The temperature was controlled with a type HHS thermostat (Shanghai, China).

Spectroelectrochemical measurements were carried out to consider absorption spectra of these polymer films under applied potentials. The spectroelectrochemical cell consisted of a quartz cell, a reference electrode of Ag/AgCl electrode, an auxiliary electrode of Pt wire, and a working electrode of polymer film modified indium tin oxide (ITO) glass. All measurements were carried out in the supporting electrolyte of CH_2Cl_2-Bu_4NPF_6 (0.10 M).

The optical density (*ΔOD*) at the specific wavelength (λ_{max}) was determined by *%T* value of electrochemically oxidized and reduced films, using the following equation:[67]

$$\Delta OD = \log\left(T_{\mathrm{ox}}/T_{\mathrm{red}}\right) \qquad (1)$$

The coloration efficiency (*CE*) is defined as the relation between the injected/ejected charge as a function of electrode area (Q_d) and the change in optical density (Δ*OD*) at the specific dominant wavelength (λ_{max}) as illustrated by the following equation (2):[68]

$$CE = \Delta OD/Q_{\mathrm{d}} \qquad (2)$$

Results and discussion

Syntheses of monomers

Using the amino group/carboxyl group of amino acids to form amide or ester bond are two main approaches to introduce amino acids into EDOT side chain. We have ever attempted to the synthesis of L-alanine-modified EDOT through esterification of 2'-hydroxymethyl-3,4-ethylenedioxythiophene (EDOT-MeOH) with L-alanine.[61] Unfortunately, after removing the Boc group on L-alanine, the obtained monomer will be hydrolyzed in short time due to the existence of its own amino group. Hence, another route was explored to efficiently synthesize EDOT-Leu in this work (Scheme 2). Firstly, EDOT-N_3 was synthesized based on a versatile intermediate of EDOT-MeCl, and then EDOT-$MeNH_2$ was obtained by reducing azide group of EDOT-N_3.[69,70] EDOT-Boc-Leu was made according to the steps described by McTiernan et al.[71] Subsequently, a common organic acid of TFA was chosen to remove Boc group on the EDOT-Boc-Leu to get EDOT-Leu monomer.

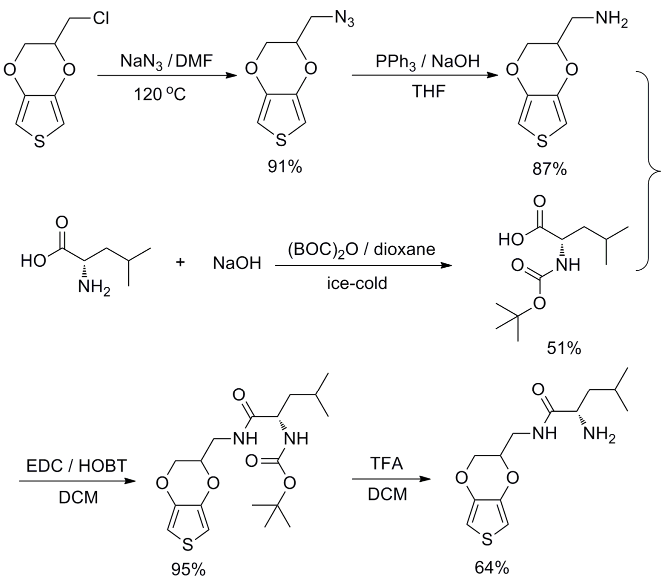

Scheme 2. Efficient synthesis routes for EDOT-Boc-Leu and EDOT-Leu.

Electrochemical polymerization of EDOT-Boc-Leu and EDOT-Leu

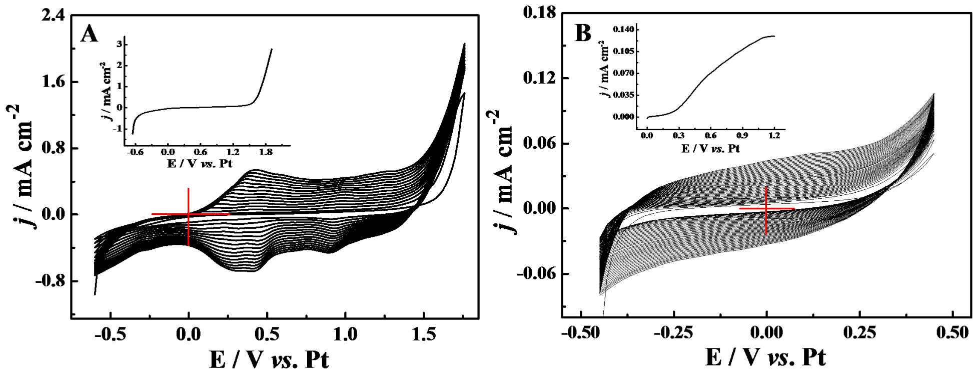

Figure 1. CVs of EDOT-Boc-Leu (A) in CH_2Cl_2–Bu_4NPF_6 (0.1 M) and EDOT-Leu (B) in CH_2Cl_2–Bu_4NPF_6 (0.1 M) containing 5% TFA. Monomers concentration: 0.01 M. Potential scan rate: 100 mV s^{-1}.

The polymers were electrosynthesized in CH_2Cl_2-Bu_4NPF_6 (0.10 M) system containing 0.01 M monomers (5% TFA were added to the monomer of EDOT-Leu mixture solutions). The addition of TFA during the electrochemical polymerization of EDOT-Leu could suppress the oxidation of amino group, and decreased the onset oxidation potential of corresponding monomer. As seen in Figure 1, all the CVs showed similar characteristics to those of other inherently conducting polymers, which indicated that the polymerization proceeded easily even at low monomer concentrations. The two insets in Figure 1 showed onset oxidation potentials of EDOT-Boc-Leu (at 1.5V) and EDOT-Leu (at 0.6 V). In the first cycle of CVs, the current density on the reverse scan was higher than that on the forward scan (in the region of -0.70 V to 1.6 V (EDOT-Boc-Leu) and -0.45 V to 0.45 V (EDOT-Leu)). In comparison with the two figures, the formation of this loop could be explained as the characteristics of nucleation process.[72-75] In Figure 1A, during the oxidative scan, two oxidation peaks appeared at 0.42 V and 1.24 V, also three reduction peaks appeared at 0.26 V, 0.43 V and 0.91 V. And in Figure 1B, the redox peaks were two relatively wide peaks. All these peaks were attributed to the *p*-doping/dedoping processes of PEDOT-Boc-Leu and PEDOT-Leu films formed in previous scans. Upon sequential cycles, the redox currents increased, implying that the formation of an electroactive and conductive layer on the Pt electrode surface (light-blue to blue-black as the deposit thickened) was gradually increasing. Moreover, the broad redox waves of the as-formed PEDOT-Boc-Leu and PEDOT-Leu films could be ascribed to the wide distribution of the polymer chain length or the version of conductive species on the polymer main chain from the dedoped state to polarons, from polarons to bipolarons, and finally from bipolarons to the metallic state.[76] The potential shift of the current wave maximum provided information about the increase of the electrical resistance of the polymer films and the overpotential needed to overcome this resistance.

Potentiostatic synthesis was employed to prepare PEDOT-Boc-Leu and PEDOT-Leu films. Considering the overall factors affecting the quality of the formed films, such as moderate polymerization rate, negligible overoxidation, regular morphology, and good adherence against the working electrode, the selected applied potential were 1.60 V and 0.75 V for the electropolymerization of EDOT-Boc-Leu and EDOT-Leu, respectively.

Infrared spectra

Vibrational spectra can provide much structural information for conducting polymers, especially for insoluble and infusible polymers. A comparison of the evolution of the vibrational modes appearing in conducting polymers and in some simpler related molecules acting as references usually facilitates the interpretation of the experimental absorption spectra. IR spectra of the monomer (a), the doped (b) and dedoped (c) polymers were illustrated in Figure 2. From these figures, no apparent difference was found between the IR spectra of the doped and dedoped polymers, which mainly due to the automatic dedoping process of polymers, concerning dopant removal. The details of the band assignments of monomers, doped polymers and dedoped polymers were given in Table 1. The peak at 3110 cm^{-1} for EDOT-Boc-Leu (Figure 2A) was produced by C–H vibration of the 2,5-positions in the thiophene ring. This peak was retained in the monomer (Figure 2A) but disappeared in the electrochemical polymerized samples (Figure 2A and 2B). This indicated that the electropolymerization of EDOT occurred at the 2,5-positions of the thiophene ring. From Figure 2 and Table 1, the C=O stretching vibration existed in the spectra of monomers and polymers, indicating that the C=O double bond was not destroyed during electrochemical polymerization.

All results confirmed that the structures of EDOT-Boc-Leu and EDOT-Leu were not destroyed during the electrochemical polymerization process. Moreover, the augmented width and shifts of these bands from the monomer to polymer manifested the occurrence of the electrochemical polymerization. The broadening of the IR bands in the experimental spectra was due to the resulting product composed of oligomers with wide chain dispersity. The vibrational peaks of the oligomers with different polymerization degrees had different IR shifts. These peaks overlapped one another and produced broad band with hyper-structures. Furthermore, there were chemical defects on the polymer chains, which resulted from the inevitable overoxidation of the polymers. This also contributed to the band broadening of IR spectra.[77]

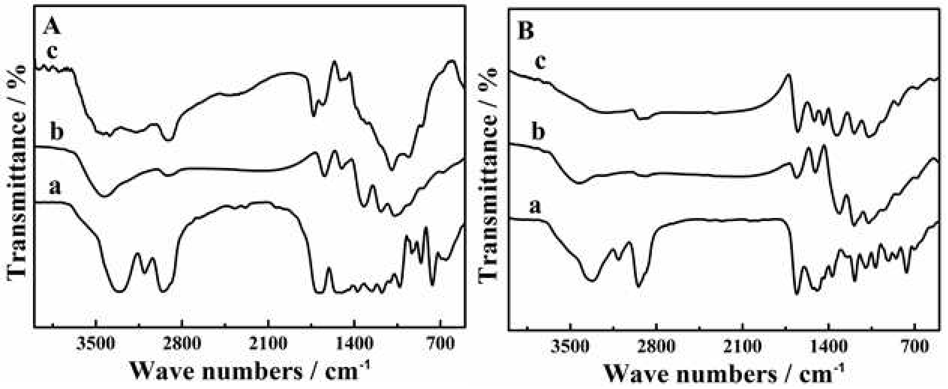

Figure 2. IR spectra of monomers and polymers: EDOT-Boc-Leu (A-a), doped PEDOT-Boc-Leu (A-b), dedoped PEDOT-Boc-Leu (A-c), EDOT-Leu (B-a), doped PEDOT-Leu (B-b) and dedoped PEDOT-Leu (B-c).

Table 1. Assignments of IR Spectra of monomers (EDOT-Boc-Leu and EDOT-Leu) and polymers (PEDOT-Boc-Leu and PEDOT-Leu)

EDOT-Boc-Leu		EDOT-Leu	
band (cm^{-1})	assignment	band (cm^{-1})	assignment
3115 (a), 1684 (a), 1553 (a), 1174 (a); 3127 (b), 1725 (b), 1513 (b), 1198 (b); 1641 (c), 1507 (c), 1298 (c)	N-H stretching vibration	3325 (a), 3428 (b), 3303 (c)	N-H stretching vibration
1728 (a), 1726 (b), 1647 (c)	C=O stretching vibration	1655 (a), 1656 (b), 1647 (c)	C=O stretching vibration

Thermal analysis

The thermal stability of conducting polymers is very essential parameter for their potential applications. It is known that the skeletal decomposition temperatures of conducting polymers are usually low, generally reported to be lower than 600 K, which hinders the practical uses of these polymers in various fields.[78] To investigate the thermal stability of PEDOT-Boc-Leu and PEDOT-Leu films, TG and DTG experiments were performed under a nitrogen stream at a heating rate of 10 K min^{-1}. As shown in Figure 3, it could be clearly observed that there were three-step weight losses for two polymers. The polymers initially underwent a small weight decrease (about 5.79% for PEDOT-Boc-Leu, and 7.34% for PEDOT-Leu) at relatively low temperature (from 286 to 410 K), which may be attributed to evaporation of trace water in the polymers. As the temperature increasing, a more pronounced weight loss step (about 43.84% for PEDOT-Boc-Leu) was observed for $410\ K < T \leq 698\ K$, which may be caused by the Boc protected L-leucine group oxidizing decomposition of the skeletal PEDOT-Boc-Leu side chain structure. And for PEDOT-Leu (about 49.23% at $410\ K < T \leq 705\ K$), the result may be caused by the L-leucine group oxidizing decomposition of the skeletal PEDOT-Leu side chain structure. With the gradual increasing of the temperature, weight went on losing (about 14.74% for PEDOT-Boc-Leu, and 11.96% for PEDOT-Leu), which were essentially due to the oxidizing decomposition of the skeletal PEDOT-Boc-Leu and PEDOT-Leu backbone chain structures. As seen in Figure 3A, B, the residual weight of PEDOT-Boc-Leu (about 35.63%) and PEDOT-Leu (about 31.47%) films, also indicated the high thermal stability of PEDOT-Boc-Leu and PEDOT-Leu films. Simultaneously, the DTG curves showed that the corresponding maximal decomposition occurred at 620 K (PEDOT-Boc-Leu film), and at 615 K (PEDOT-Leu film). Based on above discussion, both PEDOT-Boc-Leu and PEDOT-Leu exhibited good thermal stabilities.

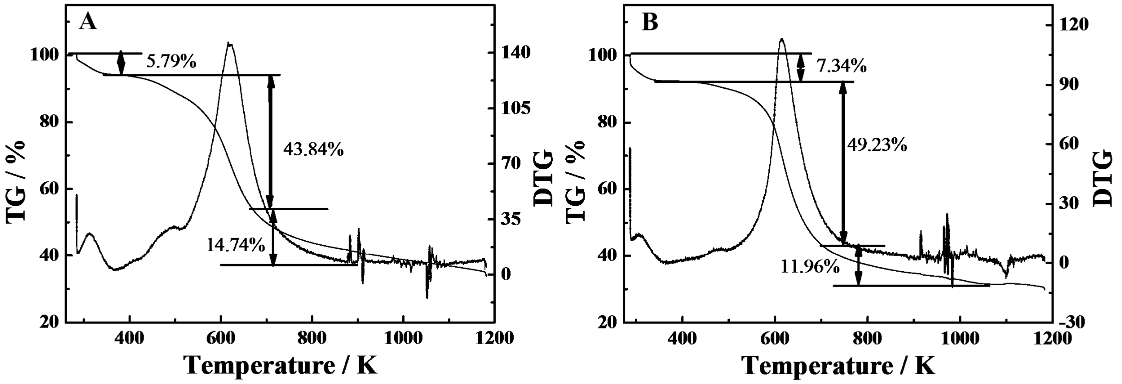

Figure 3. TG/DTG curves of dedoped PEDOT-Boc-Leu (A) and dedoped PEDOT-Leu (B) films.

CD spectra of polymer films

CD is one of the most interesting properties of chiral conducting polymers, as well as the linearly polarized dichroism. The CD of conjugated polymers originating from their chiral structure requires no macroscopic alignment of the polymers. Figure 4 showed CD spectra of PEDOT-Boc-Leu and PEDOT-Leu films. The CD peaks of all polymers from 280 nm to 320 nm were due to the single chirality of amino acid chain. A chiral carbon on the dioxane ring of EDOT was racemic before polymerization. Therefore, the polymers should not have peaks in the long wavelength. But for PEDOT-Boc-Leu, the oxygen of carbonyl on Boc group may form hydrogen bonds with the nitrogen of amide on other polymer unions or the carbonyl of amide may form hydrogen bonds with the amino group of amino acids on other polymer unions, which will induce the main chains of polymers to take a helically twisted structure and the doped and dedoped PEDOT-Boc-Leu had their peaks in the long wavelength. Meanwhile, compared with the doped PEDOT-Boc-Leu, it could be observed that the chirality of the dedoped sample was enhanced. For PEDOT-Leu, the reasons of the polymer main chains to take a helically twisted structure and their peaks in the long wavelength were that the amino group on amino acid chains may form hydrogen bonds with the nitrogen of amide on other polymer unions or the carbonyl of amide might form hydrogen bonds with the amino group of other polymer unions. And different from PEDOT-Boc-Leu, compared with the doped PEDOT-Leu, the dedoped one had another kind of enhanced CD intensity. These results demonstrated that the main chains of polymers took helically twisted structures under the introduction of the chiral amino acid side chains, and the dedoping processes were helpful to enhance the chirality of polymers. The chirality of the polymer weakened as the twisting degree decreased.[20] At the same time, the distance between the polymer main chains was expanded because the dopants (PF_6^-) were intercalated into the main chains. The increase of interchain distance weakened the helical π-stacking, causing a decrease in CD intensity.

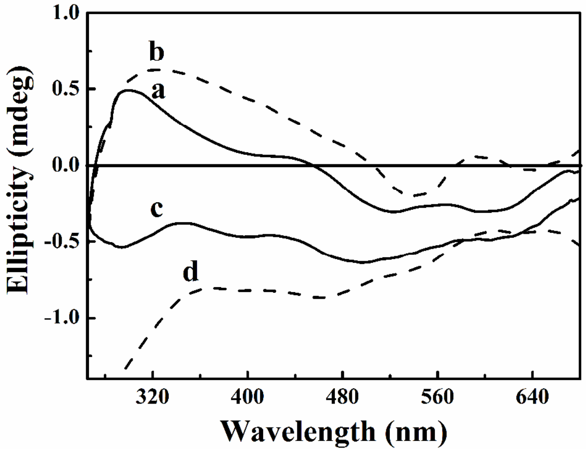

Figure 4. CD spectra of the doped PEDOT-Boc-Leu (a) and dedoped PEDOT-Boc-Leu (b), doped PEDOT-Leu (c) and

dedoped PEDOT-Leu (d). The polymers were dissolved in DMSO.

UV-vis and fluorescent spectra

PEDOT-Boc-Leu film was prepared from CH_2Cl_2–Bu_4NPF_6 in the doped state with dark brown color. While PEDOT-Leu film was prepared in CH_2Cl_2–Bu_4NPF_6 containing 5% TFA were in the doped state with dark brown color. When they were dedoped by 25% ammonia for three days, their color both changed to brownish yellow. It was very interesting that both dedoped PEDOT-Boc-Leu and PEDOT-Leu films were partly soluble in many common organic solvents, such as acetonitrile, DMSO, dichloromethane, tetrahydrofuran, and chloroform, etc.

UV–*vis* spectra of the monomers and corresponding polymer films dissolved in DMSO were illustrated in Figure 5. The monomer of EDOT-Boc-Leu showed a characteristic absorption peak at 273 nm (Figure 5A-a), while the spectra of the doped and dedoped PEDOT-Boc-Leu films showed two much broader absorptions with their maximum at 566 nm (Figure 5A-b) and 560 nm (Figure 5A-c), respectively. In comparison, EDOT-Leu monomer presented a characteristic absorption peak at 266 nm (Figure 5B-a) and the doped PEDOT-Leu film showed absorption at 570 nm (Figure 5B-b) and the dedoped PEDOT-Leu film presented absorption at 560 nm (Figure 5B-c). The overall absorption of PEDOT-Boc-Leu tailed off to more than 700 nm (Figure 5A and 5B). Generally, longer wavelength in spectra indicated longer polymer sequence.[79] These spectral results confirmed the occurrence of electrochemical polymerization among the monomer and the formation of a conjugated polymer with broad molar mass distribution.

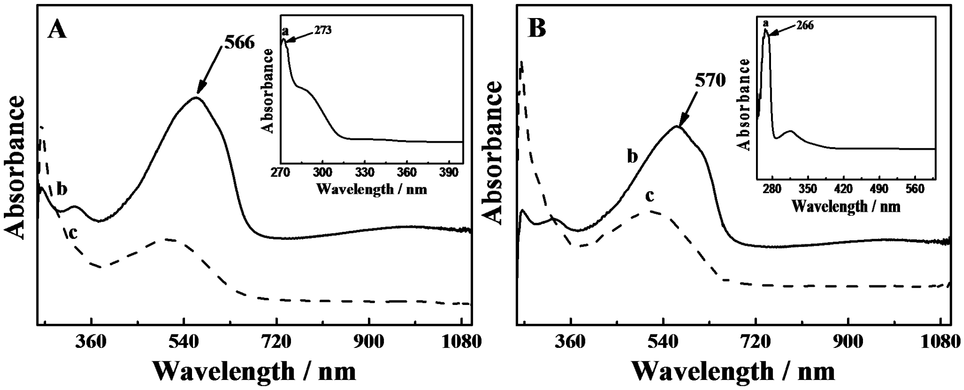

Figure 5. UV-*vis* spectra of monomers and polymers: EDOT-Boc-Leu (A-a), doped PEDOT-Boc-Leu (A-b), dedoped PEDOT-Boc-Leu (A-c), EDOT-Leu (B-a), doped PEDOT-Leu (B-b) and dedoped PEDOT-Leu (B-c). Solvent: DMSO.

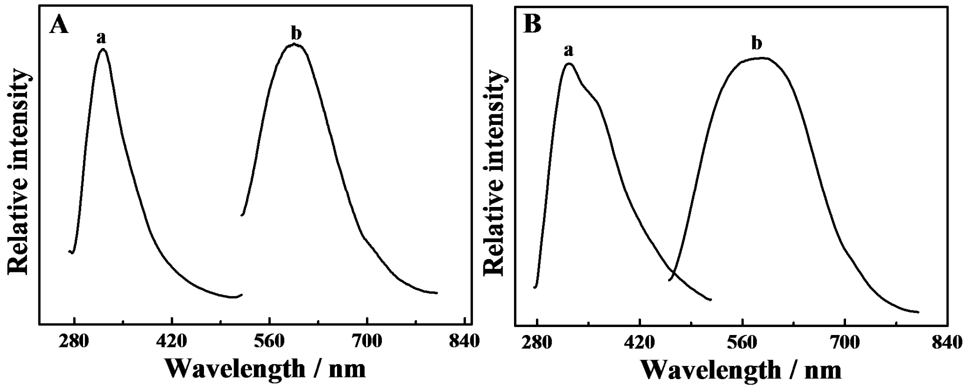

Figure 6. Fluorescence spectra of monomers and polymers: EDOT-Boc-Leu (A-a), dedoped PEDOT-Boc-Leu (A-b), EDOT-Leu (B-a), and dedoped PEDOT-Leu (B-b). Solvent: DMSO.

Surface morphology

SEM was carried out in order to study the surface morphology of the as-prepared conducting polymer films. There were obvious differences in surface morphology of the doped/dedoped PEDOT-Boc-Leu films. The doped PEDOT-Boc-Leu film surface was consisted of well-separated globules in the magnification image and the diameter of most globules was less than 1 nm (Figure 7a), which was in contrast to the smooth surface of the pristine ITO electrode. Moreover, the globular humps were found to have irregular shape in the magnification image and some particles presented in Figure 7a. However, in Figure 7b, the dedoped PEDOT-Boc-Leu film appeared to be isolated particles, quite spherical, and their sizes were also less than 1 nm in diameter. This result may be attributed to the intercalation of dopants such as PF_6^- into the interchains of PEDOT-Boc-Leu film in the doped state, while in the dedoped state PF_6^- couterions were removed during the dedoping procedure. In Figure 7c, PEDOT-Leu film in the doped state had a homogeneous, compact and smooth morphology. Simultaneously, the film of PEDOT-Leu in the dedoped state showed a swollen morphology (Figure 7d). These differences between the doped and dedoped polymer films were mainly due to the migration of counteranions out of the polymer films and their gradual solubility from the electrode to the solution during the dedoping processes,[80] which broke the relatively smooth surfaces of doped polymer films.

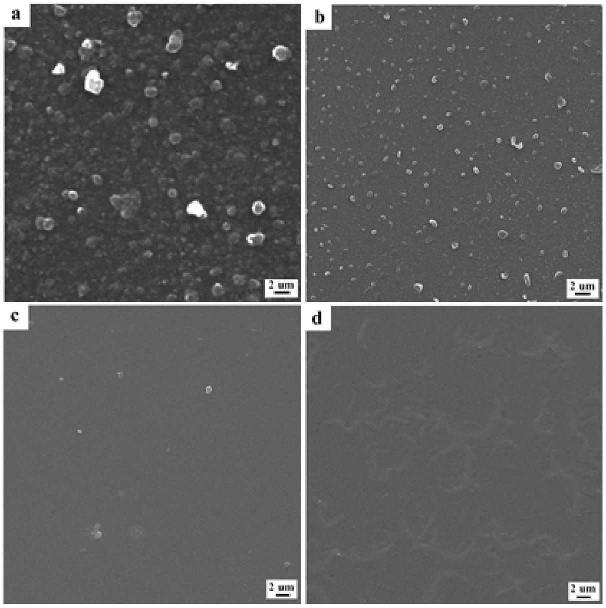

Figure 7. SEM photographs of PEDOT-Boc-Leu and PEDOT-Leu films deposited electrochemically on ITO electrode; doped and dedoped PEDOT-Boc-Leu (a and b); doped and dedoped PEDOT-Leu (c and d).

Electrochemistry of PEDOT-Boc-Leu and PEDOT-Leu films

For insight into the electroactivity of the obtained polymer films, the electrochemical behavior of PEDOT-Boc-Leu and PEDOT-Leu films-modified electrodes were investigated by cyclic voltammetry in monomer-free CH_2Cl_2–Bu_4NPF_6 (Figure 8). It was clearly seen that modified electrodes represented steady-state and broad redox peaks in selected electrolytes. This might be ascribed to the presence of slow diffusion of the counterions inside the films, changes of the films capacitance, and a wide distribution of the polymer chain length resulting from coupling defects distributed statically.[81] The peak current densities were linearly proportional to the potential scanning rates (inset in Figure 8), indicating that the redox processes were non-diffusional and the electroactive polymer films were well adhered to the working electrodes surface. Furthermore, the conversion between conducting (doped) and insulating (dedoped) state was no significant decomposition, which implied the materials had high redox stability.

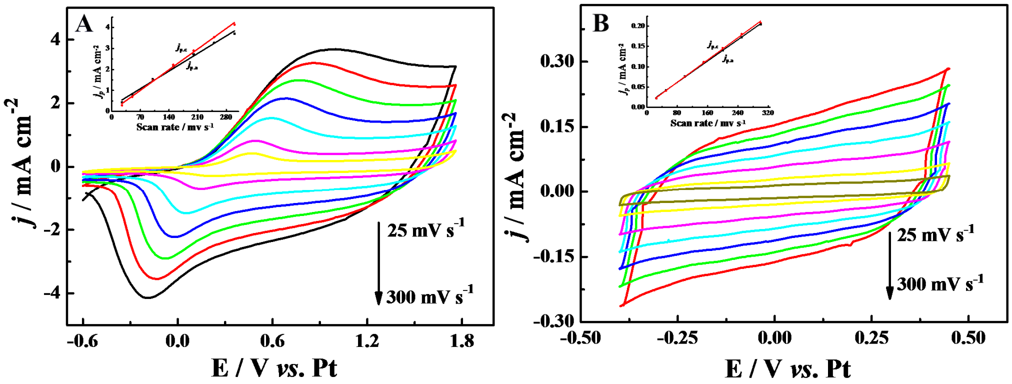

Figure 8. CVs of EDOT-Boc-Leu (A) and EDOT-Leu (B, containing 5% TFA) films in CH_2Cl_2–Bu_4NPF_6 (0.1 M) at a potential scan rates of 25, 50, 100, 150, 200, 250, and 300 mV s^{-1}. The films were obtained by CV. Inset: plots of redox peak current densities vs. potential scan rates. j_p is the peak current densities, $j_{p,a}$ and $j_{p,c}$ denote the anodic and the cathodic peak current densities, respectively.

Spectroelectrochemical properties of PEDOT-Boc-Leu and PEDOT-Leu films

Spectroelectrochemical studies of PEDOT-Boc-Leu and PEDOT-Leu films were performed to evaluate their electronic properties and band gaps, and to elucidate the effect of amino acid substitution on the electronic properties of PEDOT. As shown in Figure 9, the electrooptical properties of the polymer films were investigated using the changes of electronic absorption spectra at various applied voltages. PEDOT-Boc-Leu and PEDOT-Leu films were electrosynthsized directly on ITO glasses, and a home-made electrochemical cell was built from a commercial UV-*vis* cuvette. The cell was placed in the optical path of the sample light beam in a ultraviolet–visible–near infrared (UV–*vis*–NIR) spectrophotometer, which allowed us to acquire electronic absorption spectra under potential control in CH_2Cl_2–Bu_4NPF_6 (0.1 M) solution. As each potential was stepped, the absorption in the visible regime began to decrease, whereas that in the NIR regime increased, indicating the creation of lower energy charge carriers at the expense of π-π* transition.[82, 83] The spectroelectrochemistry of PEDOT-Boc-Leu film upon oxidation was presented in Figure 9A as a series of UV–*vis*–NIR absorbance curves and the corresponding colors of electrochemically prepared films correlated with electrode potentials. In view of the overall situation, for PEDOT-Boc-Leu, the trend of absorbance curves and the position of absorbance peaks were very similar to PEDOT. Stepwise oxidation of the polymer (increasing applied voltage from -1.0 to 1.0 V) showed the fading of absorbance at 600 nm and typical evolution of peaks at more than 730 nm.[84] In the dedoped form, the film exhibited strong absorption at the wavelength around 600 nm, approximately the same as that of PEDOT, but it was almost obvious at the wavelength more than 710 nm. The band gap (extracted from the onset of the π-π* transition) for the dedoped polymer was calculated as 1.67 eV using the absorption band centered at 745 nm, which was comparable to the reported optical band gap of parent PEDOT (1.6 eV). This implied that the pendant amino acid group had little influence on the electronic properties of PEDOT.

For a comparative study, the spectral changes of PEDOT-Leu were presented in Figure 9B. The neutral form of the PEDOT-Leu showed a distinct π-π* transition at 600 nm. Further oxidation of the polymer films, a new absorption band were observed around 950 nm due to the formation of bipolarons. Furthermore, comparable to the corresponding PEDOT, the lower band gap of PEDOT-Leu led to a lower trapping of electrons and facilitates better electron injection from the contact, so that PEDOT-Leu film required low potentials for the electrochromic switching.

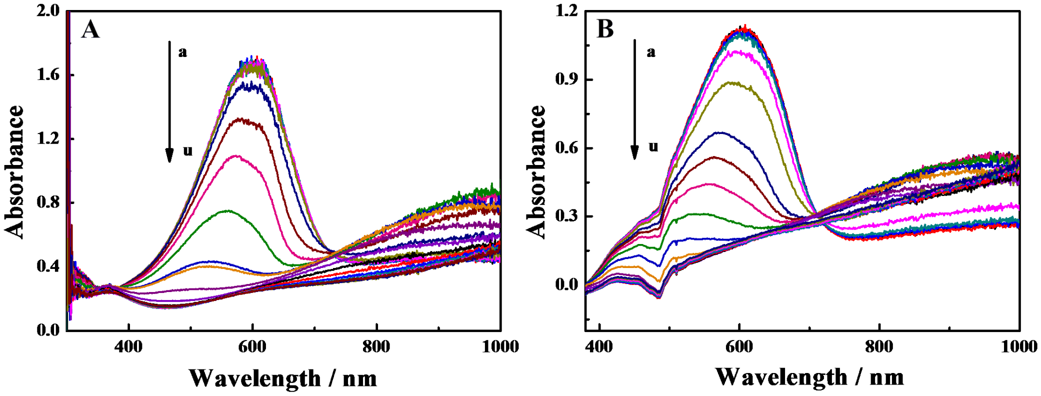

Figure 9. Spectroelectrochemistry for PEDOT-Boc-Leu (A) in CH_2Cl_2–Bu_4NPF_6 (0.1 M) and PEDOT-Leu (B) in CH_2Cl_2–Bu_4NPF_6 (0.1 M) containing 5% TFA as applied potentials between -1.0 V and 1.0 V on ITO coated glass. (a) -1.0 V, (b) -0.9V, (c) -0.8V, (d) -0.7 V, (e) -0.6 V, (f) -0.5V, (g) -0.4 V, (h) -0.3 V, (i) -0.2 V, (j) -0.1 V, (k) 0.0 V, (l) 0.1 V, (m) 0.2 V, (n) 0.3 V, (o) 0.4 V, (p) 0.5 V, (q) 0.6 V, (r) 0.7 V, (s) 0.8 V, (t) 0.9 V, (u) 1.0 V.

Electrochromic switching of PEDOT-Boc-Leu and PEDOT-Leu films

As-prepared PEDOT-Boc-Leu and PEDOT-Leu films had favorable electrochromic properties compared with PEDOT. Namely, PEDOT-Boc-Leu and PEDOT-Leu films in the doped state were dark blue and blue (Figure 10A, C), respectively. When they were dedoped by electrochemical method, their colors changed to purple and pink (Figure 10B, D). As seen in Figure 10A, B, doped and dedoped PEDOT-Boc-Leu films clearly exhibited helical structures, which were due to the function chiral amino acid group. In order to gain further insight into their electrochromic properties, the optical switching studies were investigated using a square wave potential step method coupled with optical spectroscopy known as chronoabsorptometry in a monomer-free solution. The electrochromic parameters, such as optical contrast ratio (*OD*%), response time and coloration efficiency of the polymer films were explored by increment and decrement in the transmittance with respect to time at the specific absorption wavelength of 600 nm for PEDOT-Boc-Leu and 600 and 960 nm for PEDOT-Leu (Figure 11B, C). The potentials switched stepwise between doped and dedoped states with a residence time of 10 s. The optical contrast ratio, response time and coloration efficiency of PEDOT-Boc-Leu and PEDOT-Leu films were summarized in Table 2.

The optical contrast ratios of PEDOT-Boc-Leu between dedoped (at -0.8 V) and doped states (at 0.6 V) were found to be 49% at 600 nm (Figure 11A). For PEDOT-Leu, the transmittance differences at different wavelengths were measured using a UV–*vis*–NIR spectrophotometer as the applied potential between -1.0 V and 1.0 V. The optical contrast ratios of PEDOT-Leu were showed to be 43% at 600 nm and 18% at 960 nm (Figure 11B, C).

The *CE* is also an important characteristic for electrochromic materials and obtained for a certain amount of the charge injected in the polymer as a function of the change in optical density. In this study, *CE* was measured as 163 cm^2 C^{-1} (at 600 nm) for PEDOT-Boc-Leu, while for PEDOT-Leu, the *CE* was calculated for 351 cm^2 C^{-1} at 600 nm and 431 cm^2 C^{-1} at 960 nm. Compared with PEDOT (183 cm^2 C^{-1}),[70] the *CE* of PEDOT-Leu was much higher. Response time is also an important parameter for a polymer since it indicates the speed of ions moving into the polymer chains during the doping process. Typically, for most electrochromic conducting polymers, the oxidation of the dedoped form (coloration step) proceeds more slowly than the reduction of the doped form (bleaching step) due to the difference in charge transport rates between the two states. However, the results about PEDOT-Boc-Leu and PEDOT-Leu films were not confirm to typical result in this experiment. The response required to attain 95% of total transmittance difference was found to be 2.3 s at 600 nm for PEDOT-Boc-Leu and 2.2 s at 600 nm for PEDOT-Leu from the dedoped state to the doped state, while from the doped state to the dedoped state, the response time was 2.5 s at 600 nm for PEDOT-Boc-Leu and 5.8 s at 600 nm for PEDOT-Leu, respectively.

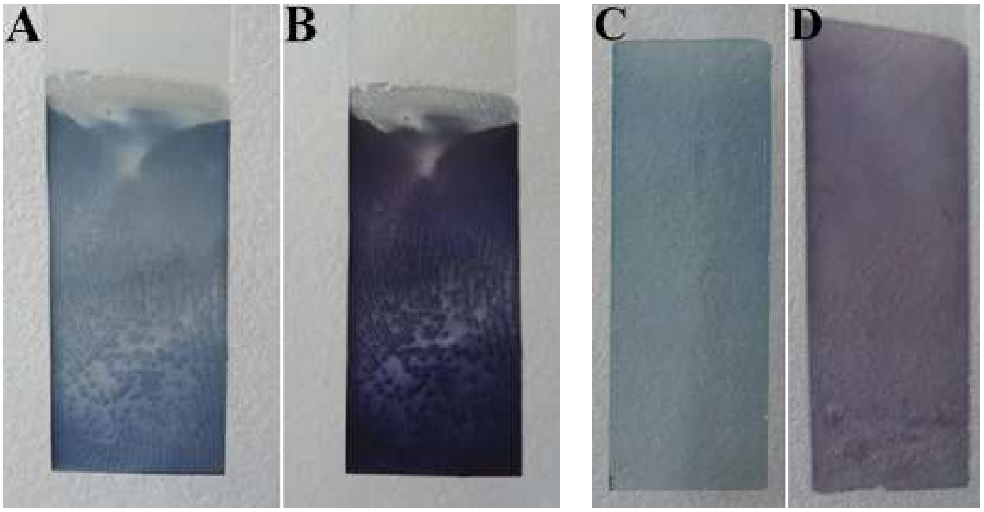

Figure 10. Photographs of PEDOT-Boc-Leu and PEDOT-Leu films deposited electrochemically on ITO electrode; doped and dedoped PEDOT-Boc-Leu (a and b); doped and dedoped PEDOT-Leu (c and d).

Table 2. Electrochromic parameters for PEDOT-Boc-Leu and PEDOT-Leu

Polymer	Wavelength / nm	T_{red} / %	T_{ox} / %	ΔT / %	response time (s)		coloration efficiency (cm^2/C)
					oxidation	reduction	
PEDOT-Boc-Leu	600	4	53	49	2.3	2.5	163
PEDOT-Leu	600	10	53	43	2.2	5.8	351
	960	45	27	18	4.2	5.8	431

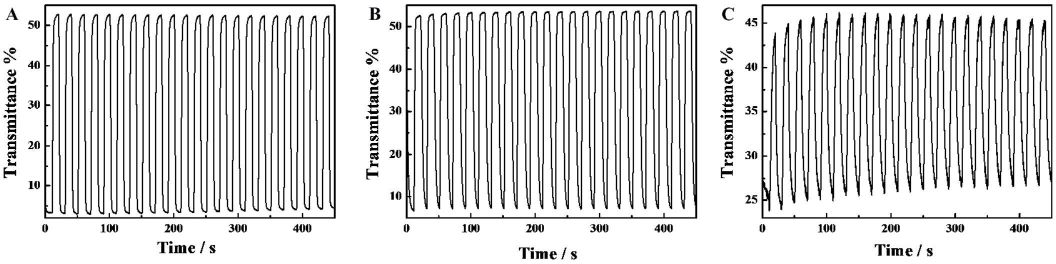

Figure 11. Electrochromic switching and optical absorbance monitored at 600 nm (A) for PEDOT-Boc-Leu recorded during double step spectrochronoamperometry between -0.8V and 0.6 V and at 600 nm (B) and 960 nm (C) for PEDOT-Leu between -1.0 V and 1.0 V for a switching time of 10 s.

Conclusions

Chiral EDOT-Boc-Leu and EDOT-Leu were firstly synthesized by some readily synthesized steps and electropolymerized for the preparation of corresponding chiral polymers in CH_2Cl_2-Bu_4NPF_6 (0.1 M) system. A series of characterizations were systematically tested for monomers and polymers. The obtained chiral PEDOT-Boc-Leu and PEDOT-Leu films showed good redox activity, excellent surface structure and high thermal stability. PEDOT side chain in the presence of chiral amino acid group can induce helical structure of PEDOT. In addition, PEDOT-Boc-Leu and PEDOT-Leu films showed favorable electrochromic performances compared with PEDOT, with high optical contrast ratio (49% at 600 nm for PEDOT-Boc-Leu), high coloration efficiency (431 cm^2 C^{-1} for PEDOT-Leu) and good optical stability. It is believed that PEDOT-Boc-Leu and PEDOT-Leu films will be promising candidates for multifunctional polymeric materials in electrochromic devices, chiral recognition and optical displays. The introduction of chiral moieties into PEDOT was demonstrated to be a useful approach for the synthesis of optically active PEDOT derivatives.

Acknowledgements

The authors would like to acknowledge the financial support of this work by the National Natural Science Foundation of China (51263010, 51303073, 51272096), Natural Science Foundation of Jiangxi Province (20122BAB216011, 20142BAB206028, 20142BAB216029), Jiangxi Science and Technology Normal University (YC2013-X03).

Notes and references

School of Pharmacy, Jiangxi Science & Technology Normal University, Nanchang, 330013, P R China

† These authors contributed equally to this work.

* Corresponding authors. Tel: +86–791–88537967; Fax: +86–791–83823320.
E-mail: duanxuemin@126.com; xujingkun@tsinghua.org.cn.

1 T. Nakano, Y. Okamoto, *Chem. Rev.* 2001, **101**, 4013–4038.

2 J. J. L. M. Cornelissen, A. E. Rowan, R. J. M. Nolte and N. A. J. M. Sommerdijk, *Chem. Rev.* 2001, **101**, 4039–4070.

3 R. J. M. Nolte, *Chem. Soc. Rev.* 1994, **23**, 11–19.

4 L. A. P. Kane-Maguire, G. G. Wallace, *Chem. Soc. Rev.* 2010, **39**, 2545–2576.

5 P. A. McCarthy, J. Y Huang, S. M. Yang, H. L. Wang, *Langmuir* 2002, **18**, 259-263.

6 J. Deng, C. Zhou, N. H. Song, *Macromolecules* 2009, **42**, 6865–6872.

7 H. F. Chow, M. K. Ng, *Tetrahedron: Asymmetry* 1996, **7**, 2251-2262.

8 M. Kaniewska, T. Sikora, R. Kataky, M. Trojanowicz, *J. Biochem. Biophys. Methods*, 2008, **70**, 261-1267.

9 J. C. Ramos, R. M. Souto-Maior, M. Navarro, *Polymer* 2006, **47**, 8095-8100.

10 M. Schwientek, S. Pleus, C. H. Hamann, *J. Electroanal. Chem.* 1999, **461**, 94-101.

11 J. Papillon, E. Schulz, S. Gélinas, J. Lessard, M. Lemaire, *Synth. Met.* 1998, **96**, 155-160.

12 (a) B. M. W. Langeveld-Voss, R. A. J. Janssen, E. W. Meijer, *J. Mol. Struct.* 2000, **521**, 285–301. (b) F. Babudri, D. Colangiuli, L. D. Bari, G. M. Farinola, O. H. Omar, F. Naso, G. Pescitelli, *Macromolecules* 2006, **39**, 5206–5212.

13 P. Emiel, A. Delmotte, R. A. J. Janssen, E. W. Meijer, *Adv. Mater.* 1997, **9**, 493–496.

14 H. Goto, K. Akagi, *Synth. Met.* 2001, **119**, 165–166.

15 (a) H. Goto, *J. Polym. Sci. Part A: Polym. Chem.* 2007, **45**, 2085–2090. (b) H. Goto, Y. S. Jeong, K. Akagi, *Macromol. Rapid Commun.* 2005, **26**, 164–167.

16 B. Y. Lu, J. K. Xu, Y. Z. Li, C. C. Liu, R. R. Yue, X. X. Sun, *Electrochim. Acta*. 2010, **55**, 2391–2397.

17 T. Tsuruta, S. Inoue, F. J. Furukawa, *Macromol. Chem.* 1965, **84**, 298–299.

18 P. E. Ebert, C. C. Price, *J. Polym. Sci.* 1959, **34**, 157–160.

19 E. Yashima, K. Maeda, Y. Okamoto, *Nature* 1999, **399**, 449–451.

20 Y. S. Jeong, K. Akagi, *Macromolecules* 2011, **44**, 2418–2426.

21 S. Matsushita, Y. S. Jeong, K. Akagi, *Chem. Commun.* 2013, **49**, 1883–1890.

22 H. Goto, K. Akagi, *Macromol. Rapid Commun.* 2004, **25**, 1482–1486.

23 H. Goto, K. Akagi, *Chem. Mater.* 2006, **18**, 255–262.

24 H. Goto, K. Akagi, *Macromolecules* 2005, **38**, 1091–1098.

25 M. Goh, M. Kyotani, K. Akagi, *J. Am. Chem. Soc.* 2007, **129**, 8519–8527.

26 T. Mori, T. Sato, M. Kyotani, K. Akagi, *Macromolecules* 2009, **42**, 1817–1823.

27 T. Mori, M. Kyotani, K. Akagi, *Macromolecules* 2010, **43**, 8363–8372.

28 M. Goh, T. Matsushita, M. Kyotani, K. Akagi, *Macromolecules* 2007, **40**, 4762–4771.

29 S. Matsushita, B. Yan, S. Yamamoto, Y. S. Jeong, and K. Akagi, *Angew. Chem. Int. Ed.* 2014, **53***, 1659-1663.*

30 J. Park, M. Goh, and K. Akagi, *Macromolecules* 2014, **47**, 2784−2795.

31 D. Iarossi, A. Mucci, F. Parenti, L. Schenetti, R. Seeber, C. Zanardi, A. Forni, M. Tonelli, *Chem. Eur. J.* 2001, **7**, 676–685.

32 M. Lemaire, D. Delabouglise, R. Garreau, A. Guy, J. Roncali, *J. Chem. Soc., Chem. Commun.* 1988, 658–661.

33 D. Kotkar, V. Joshi, P. K. Ghosh, *J. Chem. Soc., Chem. Commun*. 1988, 917–918.

34 M. M. Bouman, E. E. Havinga, R. A. J. Janssen, E. W. Meijer, *Mol. Cryst. Liq. Cryst.* 1994, **256**, 439–448.

35 (a) Bayer, A. G. Eur. Patent 1988, **339**, 340. (b) F. Jonas, L. Schrader, *Synth. Met.* 1991, **41**, 831-836. (c) G. Heywang, F. Jonas, *Adv. Mater.* 1992, **4**, 116. (d) I. Winter, C. Reece, J. Hormes, G. Heywang, F. Jonas, *Chem. Phys.* 1995, **194**, 207-213. (e) Bayer, A. G. Robert Bosch, GmbH German Patent DE 19, 627069, 1998. (f) Bayer, A. G. German Patent DE 19, 627071, 1998.

36 (a) F. Jonas, G. Heywang, W. Schmidtberg, J. Heinze, and M. Dietrich. Prior: April 22, **1988**, 339-340 (Bayer AG). (b) F. Jonas and G. Heywang. Prior: April 30, 1988, 340-512 (Bayer AG), (c) F. Jonas and G. Heywang, *Electrochim. Acta*. **1994**, *39*, 1345–1347.

37 G.-D. Wolf and F. Jonas. DE 19637018 (Bayer AG), Prior: September 12, **1996**.

38 J. Hupe, W. Kronenberg, J. Kickelhain, and D. Maier, EP 1191127 (Enthone-OMI, LPKF Laser & Electronics AG), Prior: September 26, **2000**.

39 K. Neyts, A. Real, M. Marescaux, S. Mladenovski, J. Beeckman, *J. Appl. Phys.* **2008**, *103*, 093113-1–093113-5.

40 F. Jonas, W. Krafft, and B. Muys, *Macromol. Symp*. 1**995**, *100*, 169.

41 F. Jonas and J. T. Morrison, *Synth. Met.* **1997**, *85*, 1397–1398.

42 F. Jonas and K. Lerch, *Kunststoffe* **1997**, *87*, 1401–1402.

43 M. Hüppauff, R. Sybrichs, and A. Gehring. DE 19757874, (Bosch GmbH) Prior: December 12, **1997**.

44 H. Andriessen. EP 1 231 251 A1 (Agfa-Gevaert), Prior: August 14, **2002**.

45 A. Saito. JP 2002 124391 A2 (Seiko Precision Inc.), Prior: August 8, **2000**.

46 E. L. Williams, G. E. Jabbour, Q. Wang, S. E. Shaheen, D. S. Ginley, and E. A. Schiff, *Appl. Phys. Lett.* **2005**, *87*, 223504-1–223504-3.

47 J.-G. Chen, H.-Y. Wie, and K.-C. Ho, *Sol. Energy Mater. Sol. Cells* **2007**, *91*, 1472–1477.

48 D. M. Welsh, L. J. Kloeppner, L. Madrigal, M. R. Pinto, B. C. Thompson, K. S. Schanze, K. A. Abboud, D. Powell, and J. R. Reynolds, *Macromolecules* **2002**, *35*, 6517–6525.

49 A. Cirpan, A. A. Argun, C. R. G. Grenier, B. D. Reeves, and J. R. Reynolds, *J. Mater. Chem*. **2003**, *13*, 2422–2428.

50 P. Schottland, K. Zong, C. L. Gaupp, B. C. Thompson, C. A. Thomas, I. Giurgiu, R. Hickman, K. A. Abboud, and J. R. Reynolds, *Macromolecules* **2000**, *33*, 7051–7061.

51 T. G. Bäcklund, H. G. O. Sandberg, R.. Österbacka, H. Stubb, T. Mäkelä, S. Jussila, *Synth. Met.* **2005**, *148*, 87–91.

52 G. C. Schmidt, M. Bellmann, B. Meier, M. Hambsch, K. Reuter, H. Kempa, A. C. Hübler, *Org. Electron.* **2010**, *11*, 1683–1687.

53 R. M. Walczak, J. R. Reynolds, *Adv. Mater.* **2006**, *18*, 1121–1131

54 S. Matsushita, Y. S. Jeong, K. Akagi, *Chem. Commun.* **2013**, *49*, 1883–1890.

55 K. Kawabata, H. Goto, *J. Mater. Chem.* **2012**, *22*, 23514–23524.

56 Y. Sulaiman, R. Kataky, *Analyst* **2012**, *137*, 2386–2393.

57 K. Kawabata, M. Takeguchi, H. Goto, *Macromolecules* **2013**, *46*, 2078–2091.

58 K. Kawabata, H. Goto, *J. Mater. Chem.* **2012**, *22*, 23514–23524.

59 H. Goto, K. Kawabata, *Polym. Chem.* **2011**, *2*, 1098–1106.

60 J. C. Xiao, J. L. Xu, S. Cui, H. B. Liu, S. Wang, Y. L. Li, *Org. Lett.* **2008,** *10*, 645–648.

61 B. Y. Lu, Y. Lu, Y. P. Wen, X. M. Duan, J. K. Xu, S. Chen, L. Zhang, *Int. J. Electrochem. Sci.* **2013**, *8*, 2826–2841.

62 L. Zhang, Y. P. Wen, Y. Y Yao, X. M. Duan, J. K. Xu, X. Q. Wang, *J.*

Appl. Polym. Sci. **2013**, *130*, 2660–2670.

63 J. L. Segura, R. Gómez, E. Reinold and P. Ba1uerle, *Org. Lett.* **2005**, *7*, 2345-2348.

64 A. E. Daugaard, S. Hvilsted, *Macromolecules* **2008**, *41*, 4321–4327.

65 W. S. Mungall, G. L. Greene, G. A. Heavner, R. L. Letsinger, *J. Org. Chem.* **1975**, *40*, 1659–1662.

66 A. Nikola, Nikolic, P. Beak, *Org. Synth. Coll.* **1997**, *74*, 23–28.

67 C. L. Gaupp, D. M. Welsh, R. D. Rauh, J. R. Reynolds, *Chem. Mater.* **2002**, *14*, 3964–3970.

68 B. D. Reeves, C. R. G. Grenier, A. A. Argun, A. Cirpan, T. D. McCarley, J. R. Reynolds, *Macromolecules* **2004**, *37*, 7559–7569.

69 V. Coessens, Y. Nakagawa, K. Matyjaszewski, *Polym. Bull.* **1998**, *40*, 135–142.

70 W. S. Mungall, G. L. Greene, G. A. Heavner, R. L. Letsinger, J *J. Org. Chem.* **1975**, *40*, 1659–1662.

71 C. D. McTiernan, M. Chahma, *Synth. Met.* **2011**, *161*, 1532–1536.

72 A. J. Downard, D. A. Pletcher, *J. Electroanal. Chem.* **1986**, *206*, 139–45.

73 A. J. Downard, D. A. Pletcher, *J. Electroanal. Chem.* **1986**, *206*, 147–52.

74 R. E. Noftle, D. Pletcher, *J. Electroanal. Chem.* **1987**, *227*, 229–35.

75 H. Randriamahazaka, V. Noël, C. Chevrot, *J. Electroanal. Chem.* **1999**, *472*, 103–11

76 M. Zhou, J. Heinze, *Electrochim. Acta*. **1999**, *44*, 1733–1748.

77 J. X. Zhang, C. Liu, G. Q. Shi, Y. F. Zhao, *J. Polym. Sci. Part B: Polym. Phys*. **2005**, *43*, 241–251.

78 B.Y. Lu, S. Chen, J. Wang, J. K. Xu, X. M. Duan, and M. S. Pei, *Chinese J. Chem. 2012*, *30*, 1177-1184.

79 H. J. Bowley, D. L. Gerrard, W. F. Maddams, M. R. Paton, *Makromol. Chem*., **1985**, *186*, 695–705.

80 B. Y. Lu, J. Yan, J. K. Xu, S. Y. Zhou, X. J. Hu, *Macromolecules* **2010**, *43*, 4599–4608.

81 G. Inzelt, M. Pineri, J. W. Schultze, M. A. Vorotyntsev, *Electrochim. Acta*. **2000**, *45*, 2403–2421.

82 C. W. Chang, G. S. Liou, S. H. Hsiao, *J. Mater. Chem.* **2007**, *17*, 1007–1015.

83 B. Y. Lu, S. J. Zhen, S. M. Zhang, J. K Xu and G. Q. Zhao. *Polym. Chem.* DOI: 10.1039/c4py00529e

84 Y. C. Kunga, S. H. Hsiao, *J. Mater. Chem.* **2010**, *20*, 5481–5492.